Mechanization of a scalar field theory in 1 + 1 dimensions: Bogomol'nyi-Prasad-Sommerfeld mechanical kinks and their scattering

Filip Blaschke,[1,*] Ondřej Nicolas Karpíšek,[2,†] and Lukáš Rafaj[2,‡]

[1]*Research Centre for Theoretical Physics and Astrophysics, Institute of Physics, Silesian University in Opava, Bezručovo Náměstí 1150/13, 746 01 Opava, Czech Republic*

[2]*Institute of Physics, Silesian University in Opava, Bezručovo Náměstí 1150/13, 746 01 Opava, Czech Republic*

(Received 29 May 2023; accepted 14 September 2023; published 4 October 2023)

We present an updated version of a general-purpose collective coordinate model that aims to fully map out the dynamics of a single scalar field in 1 + 1 dimensions. This is achieved by a procedure that we call a mechanization, in which we reduce the infinite number of degrees of freedom down to a finite and controllable number by chopping the field into flat segments connected via joints. In this paper we introduce two new ingredients to our procedure. The first is a manifestly Bogomol'nyi-Prasad-Sommerfeld (BPS) mechanization in which BPS mechanical kinks saturate the same bound on energy as their field-theoretic progenitors. The second is allowing the joints to switch, leading to an extended concept of the effective Lagrangian, through which we describe direct collisions of mechanical kinks and antikinks.

DOI: 10.1103/PhysRevE.108.044203

I. INTRODUCTION

Field theories in $1+1$ dimensions with disconnected vacua support topological solitons, i.e., kinks, which are stable particlelike objects. Kinks (and their higher-dimensional relatives) are relevant in many areas of contemporary physics, including cosmology, condensed matter, and particle physics [1–3].

The collisions of solitons have become a major avenue for theoretical exploration of the inner workings of nonlinear field dynamics. Indeed, during collisions, the nonlinearity is "switched on" only intermittently and with an intensity that can be tuned, among other parameters, by the initial velocities of the impactors. The ultimate goal of soliton dynamics would be the ability to predict, given the initial state of solitons and the model at hand, the outcome of any collision.

Although the kink-antikink $K\bar{K}$ scattering have been studied since the late 1970s [4–8], the true quantitative understanding of their main characteristics has been achieved only recently [9–17] (see also references in [18]). A hallmark feature of $K\bar{K}$ collisions is the bouncing phenomenon. It has been long since understood as a resonant transfer of kinetic energy to and from colliding solitons into localized modes of the field. In the case of the ϕ^4 kink, they are the shape modes residing on the kinks themselves [10], while for the ϕ^6 model, a delocalized mode emerges in between the $\bar{K}K$ pair [13].

In Fig. 1 we showcase the evolution of the central field value $\phi(x=0,t)$ as a function of time and initial velocity of the $K\bar{K}$ configuration in the ϕ^4 model. This picture demonstrates the intricate dependence of the collision's outcome on the initial velocity. More precisely, we see that the bouncing happens only in certain windows that occur below the critical velocity $v_{\text{crit}} \approx 0.26$ and above $v_{\text{min}} \approx 0.18$. In between the bouncing windows there are so-called bion chimneys where the $K\bar{K}$ pair forms a long-living quasiperiodic state that slowly decays via emission of radiation.

Both a quantitative and a qualitative understanding of this phenomenology are commonly pursued through the so-called collective coordinate model (CCM). This approach aims to reduce the infinite-dimensional dynamics of the field theory down to a few most relevant degrees of freedom. The strategy is to select a background *Ansatz*: A continuous family of curves $\phi_{\text{bkg}}(x;\{X_a(t)\})$ controlled by a given number of parameters X_a that may vary with time. For a relativistic field theory with a single scalar field, i.e.,

$$\mathcal{L} = \tfrac{1}{2}\partial_\mu\phi\partial^\mu\phi - V(\phi), \tag{1}$$

the effective Lagrangian has a generic structure

$$L_{\text{eff}} = \tfrac{1}{2}g_{ab}\dot{X}_a\dot{X}_b - U(X), \quad a,b \in \{1,\dots,N\}, \tag{2}$$

where N is the number of collective coordinates and the metric and the potential are given by the integrals

$$g_{ab} \equiv \int_{-\infty}^{\infty} dx \frac{\partial\phi_{\text{bkg}}}{\partial X_a}\frac{\partial\phi_{\text{bkg}}}{\partial X_b}, \tag{3}$$

$$U(X) \equiv \int_{-\infty}^{\infty} dx \left[\frac{1}{2}\phi_{\text{bkg}}'^2 + V(\phi_{\text{bkg}})\right]. \tag{4}$$

The utility of the CCM encoded in L_{eff} depends very sensitively on ϕ_{bkg}. Regarding the strategies for selecting viable *Ansätze*, we may postulate two complementary philosophies: (i) the engineering approach and (ii) the agnostic approach.

The engineering approach, as the name suggests, relies on incorporating prior information into ϕ_{bkg}. If the goal is the analysis of $K\bar{K}$ scattering, for instance, the *Ansatz* typically

*filip.blaschke@physics.slu.cz
†karponius@gmail.com
‡lukasrafaj@gmail.com

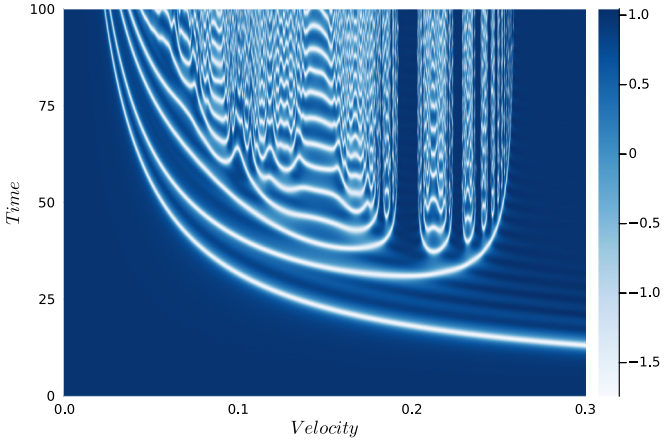

FIG. 1. Evolution of the center field value $\phi(x=0,t)$ of $K\bar{K}$ configuration for a range of initial velocities in the ϕ^4 model.

consists of a superposition of kink and antikink solutions plus a selected number of normal modes, a route that has been applied, e.g., for the ϕ^4 model [9,10] (see [18] for the somewhat intricate history of its deployment). However, CCMs that have been proposed also include Derrick modes [11], quasinormal modes [19], and/or delocalized modes [13,20,21]. In fact, the engineering approach has become a precision tool for predicting major features of the $K\bar{K}$ scattering, such as the critical velocity [17].

Despite its successes, the engineering approach has also disadvantages. In this approach, a given CCM is like a microscope that has been carefully trained on a particular spot of the sample. Regardless of how successfully a CCM models the selected feature of dynamics, it has no direct applicability to other aspects, nor can it be used for discovering new dynamical features or to unearth connections between known ones. In short, an engineering CCM is, by construction, a single-purpose tool.

On the other hand, the agnostic approach aims to be a general-purpose tool. Rather than carefully constraining the field(s) into a premeditated scope, the agnostic CCM attempts to capture rough features of the field dynamics in a coarse-grained setting. In this regard, it is mainly a tool for exploration. In practice, the best approach is a judicious synthesis of the two: Deployment of the agnostic CCM should be followed by an engineering one. Indeed, the findings of the former can be *a posteriori* verified and developed by the latter. Ideally, such a combination may allow exhaustive exploration of soliton dynamics in situations, where there is a vast space of initial configurations involving multiple fields and a higher number of spatial dimensions, which makes numerical solutions of field theory very time consuming.

To achieve this, we must first develop a toolkit for agnostic CCMs in various field theories, starting with a single scalar field in $1+1$ dimensions. An agnostic CCM must be exhaustive, meaning that the background *Ansatz* $\phi_{\rm bkg}$ approaches the continuum field in the limit $N\to\infty$. Furthermore, it must be algebraically tractable: The number of terms in the effective Lagrangian should grow linearly with N. This is to ensure that stepping from N to $N+1$ does not generate an exponential increase in complexity.

In our previous paper [22] we proposed an early candidate for such an agnostic CCM that we have dubbed mechanization. The idea is to replace a continuum field with a piecewise linear function: A mechanical field.[1] We have cataloged basic features of mechanical-field dynamics for a few lowest values of N, which is the number of nonflat segments connected by $N+1$ joints.

The most apparent advantage of the mechanization procedure is that it allows progressive exploration of the dynamics. As N increases, more modes of behavior become possible.

At $N=1$, the mechanical field is a mechanical analog of the kink: A mechanical kink (see Fig. 4). Let us point out two of its salient features: (i) A static mechanical kink can be boosted, despite the explicit breakdown of the Lorentz invariance that is typical for most CCMs, and (ii) the mechanical kink has an exact periodic solution, the so-called Derrick mode. In fact, the structure of the effective Lagrangian turns out to be virtually identical to a field-theoretic relativistic CCM for a kink [11].

At $N=2$, the mechanical field connecting the same vacua behaves as a quasiperiodic oscillator that can decay; the joints fly to opposite infinities while the mechanical field settles on the vacuum exponentially fast. In [22] we investigated how the lifetime of this mechanical oscillon depends on its initial dimensions. More importantly, we have shown that higher-N mechanical oscillons can decay via multiple channels, including disintegration into an excited pair of a mechanical kink and an anti-mechanical-kink that, before escaping to infinity, may undergo several bounces.

Although our findings were encouraging, we have also identified several shortcomings of mechanization as proposed in [22]. For example, the moduli space of a generic mechanical field turned out to be geodetically incomplete, having multiple singularities corresponding to situations when joints overlap. Further, we have also encountered a technical issue that prevented us from direct investigation of mechanical-$K\bar{K}$ scattering. Because the segment between a mechanical-$K\bar{K}$ pair lies precisely in a vacuum, there is no force between them, unlike in the field theory, where a short-range attractive force exists due to overlapping tails of kinks. Thus, a direct scattering of mechanical kinks seemed to be impossible, while scattering of approximate mechanical kinks turned out to be riddled with numerical instabilities and the presence of long-range forces.

In this paper we present a solution to the above issues in addition to other conceptual advancements. Hence, we provide a significant step towards the construction of a truly general-purpose CCM.

Our main findings are distributed in the paper as follows. In Sec. II we reintroduce the mechanization procedure and provide explicit formulas for the effective Lagrangian using two different sets of coordinates. More importantly, we define a concept of Bogomol'nyi-Prasad-Sommerfeld (BPS) mechanization that allows the construction of Bogomol'nyi-Prasad-Sommerfeld equations for static mechanical kinks

[1]Let us stress that this is an *ad hoc* choice, which has the merit of producing the simplest effective Lagrangians. Other piecewise functions could be considered. See the discussion in Sec. V.

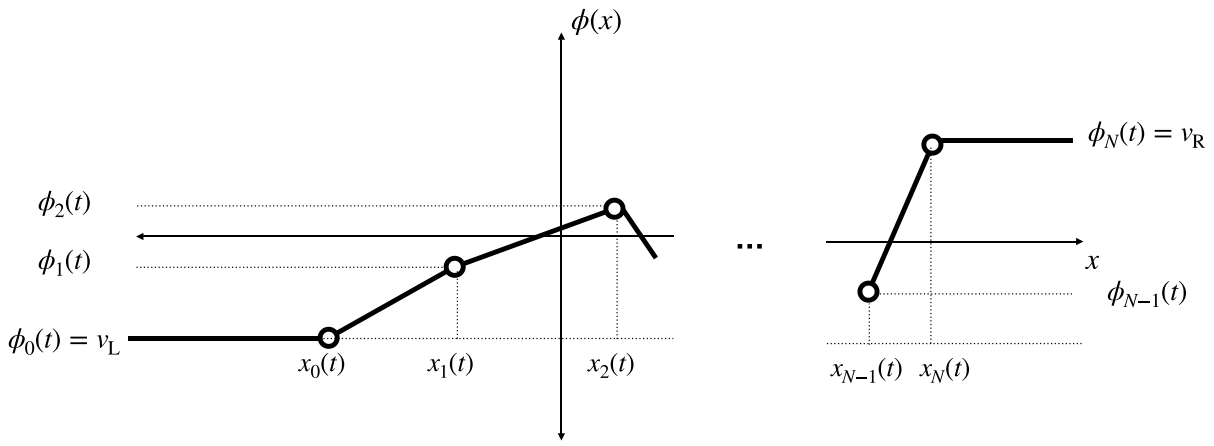

FIG. 2. Depiction of a mechanical field $\phi_M(x,t)$ as a sequence of N straight stretchable segments connected via massless joints.

saturating the same Bogomol'nyi bound [23] as field-theoretic kinks. In Sec. III we compare the properties of mechanical kinks based on non-BPS and BPS mechanization, including the discussion of normal modes. Section IV contains an investigation of direct mechanical-$K\bar{K}$ scatterings for the simplest mechanical fields. We first present a resolution of the decoupling problem: This is accomplished via loose order mechanization (LOM). In short, we show that short-range interactions of kinks in a field theory are replaced by contact interactions between mechanical kinks. By allowing the joints to pass through each other (without encountering any singularities) we continue the free dynamics of a mechanical-$K\bar{K}$ pair into to different stage, where it becomes a mechanical oscillon. This mechanical oscillon may either decay or again form a new mechanical-$K\bar{K}$ pair, which can fly apart or undergo bouncing. In this way, we show that both key features, namely, bouncing and (mechanical-)bion formation, are represented even in the simplest mechanical-$K\bar{K}$ scatterings. We showcase numerical results for both non-BPS and BPS kinks in the ϕ^4 model. Finally, in Sec. V we discuss the presented results and point out future directions for the mechanization program.

II. MECHANIZATION

In this section we gather all the technical aspects of the mechanization procedure; we define the mechanical field and discuss associated moduli space, providing explicit formulas for the metric via two complementary choices of coordinates. Finally, we provide an explicit form for the effective Lagrangian for both non-BPS and BPS approaches.

A. Mechanical field

The mechanization procedure replaces a continuous field $\phi(x,t)$ by a piecewise linear function that is defined by a set of $N+1$ control points (or joints) in the ϕ-x plane, i.e., $\{x_a, \phi_a\}$, $a = 0, \ldots, N$ (see Fig. 2). We define a mechanical field $\phi_M(x,t)$ by the formula

$$\phi_M(x,t) \equiv \sum_{a=-1}^{N} \left(\frac{\Delta\phi_a(t)}{\Delta x_a(t)}[x - x_a(t)] + \phi_a(t) \right) \chi_a. \tag{5}$$

Here $\Delta f_a(t) \equiv f_{a+1}(t) - f_a(t)$ and χ_a is the indicator function for each segment,

$$\chi_a \equiv \theta(x - x_a) - \theta(x - x_{a+1}) = -\Delta\theta(x - x_a), \tag{6}$$

where $\theta(x)$ is the Heaviside step function, i.e., $\theta(x) = 1$ if $x > 0$ and $\theta(x) = 0$ otherwise.

The $x_a(t)$ are the positions of the joints on the x axis. Note that the ϕ_a correspond to the values of the field at the ath joint, i.e., $\phi_a(t) \equiv \phi(x_a(t))$, only if they are canonically ordered, namely, $x_0(t) < x_1(t) < \cdots < x_N(t)$. Throughout this section, we assume that this ordering holds.

We impose boundary conditions on a mechanical field so that it has finite energy. Specifically, we fix the two outermost segments in some vacua, i.e., $\phi_{-1} = \phi_0 = v_L$ and $\phi_N = \phi_{N+1} = v_R$, where $v_{L,R}$ represent vacuum values on the left or right, respectively. We have formally added two static joints at spatial infinities, namely, $x_{-1} = -\infty$ and $x_{N+1} = +\infty$. The continuity of the mechanical field can be then verified by direct differentiation

$$\partial_x \phi_M(x,t) = \sum_{a=-1}^{N} \frac{\Delta\phi_a(t)}{\Delta x_a(t)} \chi_a - \sum_{a=-1}^{N} \Delta[\delta(x - x_a)\phi_a]. \tag{7}$$

The second term on the right-hand side vanishes due to the fundamental theorem of discrete calculus, i.e.,

$$\begin{aligned} \sum_{a=-1}^{N} \Delta[\delta(x - x_a)\phi_a] &= \phi_{N+1}\delta(x - x_{N+1}) - \phi_{-1}\delta(x - x_{-1}) \\ &= v_R\delta(x - \infty) - v_L\delta(x + \infty) \\ &= v_R\delta(-\infty) - v_L\delta(\infty) = 0. \end{aligned}$$

A similar argument can be made to show that $\partial_t \phi_M(x,t)$ is free of δ functions too. There are $N-1$ heights of joints $\phi_1, \ldots, \phi_{N-1}$ together with $N+1$ positions $x_0, \ldots, x_N$, totaling $2N$ degrees of freedom to describe a mechanical field with $N+1$ joints.

For further purposes, let us also introduce an alternative parametrization

$$\phi_M(x,t) \equiv \sum_{a=-1}^{N} [k_a(t)x + \Phi_a(t)]\chi_a. \tag{8}$$

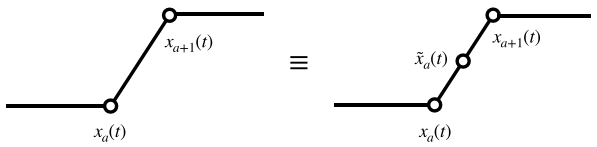

FIG. 3. Illustration of a degeneracy of $\{x_a(t), \phi_a(t)\}$ coordinates. The insertion of a new joint on any segment does not change the mechanical field.

Here the k_a are the slopes of the segments, i.e.,[2]

$$k_a \equiv \frac{\phi_{a+1} - \phi_a}{x_{a+1} - x_a}, \tag{9}$$

while the Φ_a are given as

$$\Phi_a \equiv \frac{x_{a+1}\phi_a - x_a\phi_{a+1}}{x_{a+1} - x_a}. \tag{10}$$

The boundary conditions read

$$k_{-1} = k_N = 0, \quad \Phi_{-1} = v_{\mathrm{L}}, \quad \Phi_N = v_{\mathrm{R}}. \tag{11}$$

The inverse formulas to (9) and (10) are given as

$$x_{a+1} = -\frac{\Phi_{a+1} - \Phi_a}{k_{a+1} - k_a}, \quad \phi_{a+1} = \frac{k_{a+1}\Phi_a - k_a\Phi_{a+1}}{k_{a+1} - k_a}. \tag{12}$$

The $\{k_a, \Phi_a\}$ coordinates offer some advantages over $\{x_a, \phi_a\}$. For example, the metric, discussed in the next section, has the simplest form. A more subtle issue is the redundancy (or degeneracy) of $\{x_a, \phi_a\}$ coordinates. We illustrate this in Fig. 3: If we artificially add a joint on any segment while keeping the neighboring slopes the same, the mechanical field does not change, i.e., the new joint is not dynamical. In particular, a vacuum configuration, i.e., $\phi_M = v$, can be described with a single segment, two segments, or any number of segments, with the positions $\{x_a\}$ undetermined by the dynamics for any N. This can be seen directly from the formula (5) by setting $\phi_0 = \cdots = \phi_N = v$.

In $\{k_a, \Phi_a\}$ coordinates, on the other hand, the vacuum is given by $k_0 = \cdots = k_N = 0$ and $\Phi_0 = \cdots = \Phi_N = v$ and there are no undetermined degrees of freedom. Furthermore, there is truly only a single segment, because whenever two subsequent Φ_a and k_a equal each other, the x_a is undefined through Eq. (12). This is most easily seen from the rewriting of (8) as

$$\phi_M(x,t) \equiv v_{\mathrm{L}} + \sum_{a=0}^{N} \theta(x - x_a(t))[\Delta k_a(t)x + \Delta\Phi_a(t)], \tag{13}$$

which shows that whenever $\Delta k_a = \Delta\Phi_a = 0$, the coordinate x_a disappears.

B. Moduli space

Generically, for any set of collective coordinates $\{X_a\}$ the metric is given as

$$g(\{X\})_{ab} \equiv \int_{-\infty}^{\infty} dx \frac{\partial\phi}{\partial X_a}\frac{\partial\phi}{\partial X_b}. \tag{14}$$

In the $\{x_a, \phi_a\}$ coordinates, the metric consists of $(N+1)\times(N+1)$, $(N+1)\times(N-1)$, and $(N-1)\times(N-1)$ tridiagonal blocks, namely,

$$g(\{x,\phi\}) = \begin{pmatrix} g^{xx} & g^{x\phi} \\ g^{\phi x} & g^{\phi\phi} \end{pmatrix}, \tag{15}$$

where $g^{\phi x} = (g^{x\phi})^T$ and

$$g^{xx} = \begin{pmatrix} \frac{(\Delta\phi_0)^2}{3\Delta x_0} & \frac{(\Delta\phi_0)^2}{6\Delta x_0} & 0 & \cdots \\ \frac{(\Delta\phi_0)^2}{6\Delta x_0} & \frac{(\Delta\phi_0)^2}{3\Delta x_0} + \frac{(\Delta\phi_1)^2}{3\Delta x_1} & \frac{(\Delta\phi_1)^2}{6\Delta x_1} & \cdots \\ 0 & \frac{(\Delta\phi_1)^2}{6\Delta x_1} & \frac{(\Delta\phi_1)^2}{3\Delta x_1} + \frac{(\Delta\phi_2)^2}{3\Delta x_2} & \cdots \\ \vdots & \vdots & \vdots & \ddots \end{pmatrix}, \tag{16}$$

$$g^{x\phi} = \begin{pmatrix} (\phi_0 - \phi_1)/6 & 0 & 0 & \cdots \\ (\phi_0 - \phi_2)/3 & (\phi_1 - \phi_2)/6 & 0 & \cdots \\ (\phi_1 - \phi_2)/6 & (\phi_1 - \phi_3)/3 & (\phi_2 - \phi_3)/6 & \cdots \\ 0 & (\phi_2 - \phi_3)/6 & (\phi_2 - \phi_4)/3 & \cdots \\ \vdots & \vdots & \vdots & \ddots \end{pmatrix}, \tag{17}$$

$$g^{\phi\phi} = \begin{pmatrix} (x_2 - x_0)/3 & (x_2 - x_1)/6 & 0 & \cdots \\ (x_2 - x_1)/6 & (x_3 - x_1)/3 & (x_3 - x_2)/6 & \cdots \\ 0 & (x_3 - x_2)/6 & (x_4 - x_2)/3 & \cdots \\ \vdots & \vdots & \vdots & \ddots \end{pmatrix}. \tag{18}$$

The determinant reads[3]

$$|g(\{x,\phi\})| = \frac{1}{12^N}\prod_{a=-1}^{N-1}(k_{a+1} - k_a)^2 \prod_{b=0}^{N-1}(x_{b+1} - x_b)^2. \tag{19}$$

In these coordinates the metric is degenerate, i.e., $|g| = 0$, not only when positions of neighboring joints coincide, namely, $\Delta x_a = 0$, but also when subsequent slopes are equal: $\Delta k_a = 0$. The latter type of singularity reflects the aforementioned degeneracy.

On the other hand, in $\{k_a, \Phi_a\}$ coordinates, the metric consists of four $N \times N$ diagonal blocks

$$g(\{k,\Phi\}) = \begin{pmatrix} g^{kk} & g^{k\Phi} \\ g^{\Phi k} & g^{\Phi\Phi} \end{pmatrix}, \tag{20}$$

[2]Here the notation is slightly different from our previous paper [22], where we wrote k_{a+1} instead.

[3]Note that the formula for the determinant given in our previous paper [22] was written incorrectly.

where $g^{\Phi k} = g^{k\Phi}$ and

$$g^{kk} = \frac{1}{3}\begin{pmatrix} x_1^3 - x_0^3 & 0 & 0 & \cdots \\ 0 & x_2^3 - x_1^3 & 0 & \cdots \\ 0 & 0 & x_3^3 - x_2^3 & \cdots \\ \vdots & \vdots & \vdots & \ddots \end{pmatrix}, \tag{21}$$

$$g^{k\Phi} = \frac{1}{2}\begin{pmatrix} x_1^2 - x_0^2 & 0 & 0 & \cdots \\ 0 & x_2^2 - x_1^2 & 0 & \cdots \\ 0 & 0 & x_3^2 - x_2^2 & \cdots \\ \vdots & \vdots & \vdots & \ddots \end{pmatrix}, \tag{22}$$

$$g^{\Phi\Phi} = \begin{pmatrix} x_1 - x_0 & 0 & 0 & \cdots \\ 0 & x_2 - x_1 & 0 & \cdots \\ 0 & 0 & x_3 - x_2 & \cdots \\ \vdots & \vdots & \vdots & \ddots \end{pmatrix}. \tag{23}$$

Furthermore, the determinant reads

$$|g(\{k, \Phi\})| = \frac{1}{12^N}\prod_{a=0}^{N-1}(x_{a+1} - x_a)^4 \tag{24}$$

and contains only a singularity of the type $\Delta x_a = 0$.

C. Effective Lagrangian and BPS mechanization

To obtain an effective Lagrangian we insert a mechanical field given by either (5) or (8) into a Lagrangian density $\mathcal{L}$ taken as a generic scalar-field theory in $1+1$ dimensions, i.e.,

$$\mathcal{L} = \tfrac{1}{2}\dot{\phi}^2 - \tfrac{1}{2}\phi'^2 - V(\phi), \tag{25}$$

and integrate it over the x axis

$$L_{\text{eff}} = \int_{-\infty}^{\infty} dx\, \mathcal{L}(\phi_M). \tag{26}$$

The result derived by assuming canonical ordering of joints, $x_0 < x_1 < \cdots < x_N$, reads (see the details in [22])

$$\begin{aligned} L[\{x, \phi\}] &= \sum_{a=0}^{N-1}\Delta x_a\left[\frac{1}{6}\left(\Delta\dot{\phi}_a - \frac{\Delta\dot{x}_a}{\Delta x_a}\Delta\phi_a\right)^2 - \frac{\Delta\phi_a^2}{2\Delta x_a^2}\right. \\ &\quad \left. + \frac{1}{2}\left(\dot{\phi}_{a+1} - \frac{\Delta\phi_a}{\Delta x_a}\dot{x}_{a+1}\right)\left(\dot{\phi}_a - \frac{\Delta\phi_a}{\Delta x_a}\dot{x}_a\right) - \frac{\Delta\mathcal{V}(\phi_a)}{\Delta\phi_a}\right]. \end{aligned} \tag{27}$$

In the $\{k, \Phi\}$ coordinates, the same can be expressed slightly more compactly as

$$\begin{aligned} L[\{k, \Phi\}] = \sum_{a=0}^{N-1}\left(\frac{x_{a+1}^3 - x_a^3}{6}\dot{k}_a^2 + \frac{x_{a+1}^2 - x_a^2}{2}\dot{k}_a\dot{\Phi}_a + \frac{\Delta x_a}{2}\dot{\Phi}_a^2\right. \\ \left. - \frac{1}{2}k_a^2\Delta x_a - \Delta x_a\frac{\Delta\mathcal{V}(\phi_a)}{\Delta\phi_a}\right), \end{aligned} \tag{28}$$

where x_a and ϕ_a are understood as functions of k_a and Φ_a through the relations (12). In both formulas (27) and (28), $\mathcal{V}(\phi)$ is the primitive function of the potential $V(\phi)$, i.e., $\mathcal{V}'(\phi) = V(\phi)$.

Let us stress that (27) and (28) are valid only if $x_0 < x_1 < \cdots < x_N$. We will return to this point in Sec. IV, where we present the effective Lagrangian (LOM) that incorporates all possible orderings.

Let us now point out that mechanization of the potential term, i.e.,

$$\int_{-\infty}^{\infty} dx\, V(\phi_M) = \sum_{a=0}^{N-1}\Delta x_a\frac{\Delta\mathcal{V}(\phi_a)}{\Delta\phi_a}, \tag{29}$$

obtained by a direct integration is not unique and may not be the most optimal for studying topological solutions. In the following, let us label the outcome (29) a non-BPS mechanization for reasons that will become obvious.

Now let us consider a field theory in the form

$$\mathcal{L}_J = \tfrac{1}{2}\partial_\mu\phi\partial^\mu\phi + \tfrac{1}{2}J^2 + JW(\phi), \tag{30}$$

where $W(\phi)$ is the superpotential, i.e., $V(\phi) \equiv \frac{1}{2}W^2(\phi)$, and J is an auxiliary field. Of course, $\mathcal{L}_J$ is physically equivalent to (25), as can be seen by eliminating J through its equation of motion $J = -W(\phi)$ and plugging it back in.

However, if we first mechanize the auxiliary field as

$$J_M = \sum_{a=0}^{N-1}[\theta(x - x_a(t)) - \theta(x - x_{a+1}(t))]J_a(t), \tag{31}$$

where the positions of joints $x_a(t)$ are the same as those appearing in ϕ_M, inserting both J_M and ϕ_M into $\mathcal{L}_J$ and integrating over x yields

$$\begin{aligned} L_M^J &\supset \int_{-\infty}^{\infty} dx\left[\frac{1}{2}J_M^2 + J_M W(\phi_M)\right] \\ &= \sum_{a=0}^{N-1}\left(\frac{\Delta x_a}{2}J_a^2 + \Delta x_a J_a\frac{\mathcal{W}(\phi_{a+1}) - \mathcal{W}(\phi_a)}{\phi_{a+1} - \phi_a}\right), \end{aligned} \tag{32}$$

where $\mathcal{W}$ is a primitive function of the superpotential, i.e., $\mathcal{W}' = W$.

Eliminating all J_a via their equations of motion, we arrive at what we dub BPS mechanization, namely,

$$L_M^J \xrightarrow[J_a = -\Delta\mathcal{W}_a/\Delta\phi_a]{} L_M^{\text{BPS}} \tag{33}$$

$$\begin{aligned} L_M^{\text{BPS}} \equiv \sum_{a=0}^{N-1}\left[\frac{x_{a+1}^3 - x_a^3}{6}\dot{k}_a^2 + \frac{x_{a+1}^2 - x_a^2}{2}\dot{k}_a\dot{\Phi}_a + \frac{\Delta x_a}{2}\dot{\Phi}_a^2\right. \\ \left. - \frac{1}{2}k_a^2\Delta x_a - \frac{\Delta x_a}{2}\left(\frac{\Delta\mathcal{W}(\phi_a)}{\Delta\phi_a}\right)^2\right]. \end{aligned} \tag{34}$$

In other words, we have found that the following loop does not close (the horizontal arrows $\xrightarrow[M]{}$ denote mechanization, while the vertical arrows denote elimination of auxiliary variables):

$$\begin{array}{ccc} \mathcal{L}_J & \xrightarrow[M]{} & L_M^J \\ \Big\downarrow{\scriptstyle J=-W} & & \Big\downarrow{\scriptstyle J_a=-\frac{\Delta\mathcal{W}_a}{\Delta\phi_a}} \\ \mathcal{L} & \xrightarrow[M]{} & L_M \neq L_M^{\text{BPS}} \end{array} \tag{35}$$

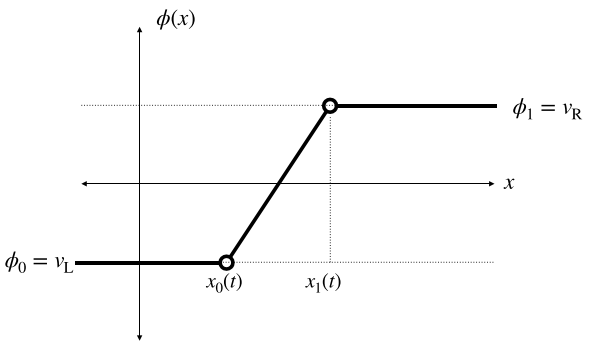

FIG. 4. Simplest mechanical model of a kink equal to a mechanical kink.

Although the difference between L_M and $L_M^{\rm BPS}$ is isolated only to the potential term and, at first glance, does not seem significant, we will show that it has a profound impact on the nature of static solutions and their dynamics.

III. STATIC SOLUTIONS

In this section we study the properties of static solutions of both L_M and $L_M^{\rm BPS}$ and highlight their differences.

A. Non-BPS mechanical kinks

To find static solutions of a generic N mechanical field we minimize the static energy

$$E_M = \sum_{a=0}^{N-1} \left(\frac{(\Delta\phi_a)^2}{2\Delta x_a} + \Delta x_a \frac{\Delta \mathcal{V}(\phi_a)}{\Delta \phi_a} \right). \tag{36}$$

The coordinates of the joints (up to overall position) can be found as[4]

$$\Delta x_a = \frac{(\Delta\phi_a)^{3/2}}{\sqrt{2[\mathcal{V}(\phi_{a+1}) - \mathcal{V}(\phi_a)]}}. \tag{37}$$

On the other hand, the field values ϕ_a follow from minimization of (36) after inserting (37), i.e.,

$$E_M \underset{(37)}{\longrightarrow} \sum_{a=0}^{N-1} \sqrt{2\Delta\phi_a[\mathcal{V}(\phi_{a+1}) - \mathcal{V}(\phi_a)]}. \tag{38}$$

This leads to a system of nonlinear algebraic equations

$$V(\phi_a)^2 = \frac{\mathcal{V}(\phi_{a+1}) - \mathcal{V}(\phi_a)}{\phi_{a+1} - \phi_a} \frac{\mathcal{V}(\phi_a) - \mathcal{V}(\phi_{a-1})}{\phi_a - \phi_{a-1}}. \tag{39}$$

The simplest solution is the $N = 1$ mechanical kink (see Fig. 4). Its static width R_K and static energy m_K are given by

$$R_K = \frac{v_R - v_L}{\sqrt{2\kappa}}, \quad m_K = (v_R - v_L)\sqrt{2\kappa}, \tag{40}$$

[4]Here we assume that the sequence $\{\phi_0, \phi_1, \ldots\}$ is monotonically increasing, i.e., the solution is a mechanical kink interpolating vacua $v_L < v_R$. The anti-mechanical-kinks would be found analogously after the appropriate insertion of absolute values inside the square roots so that $\Delta x_a > 0$ for all segments.

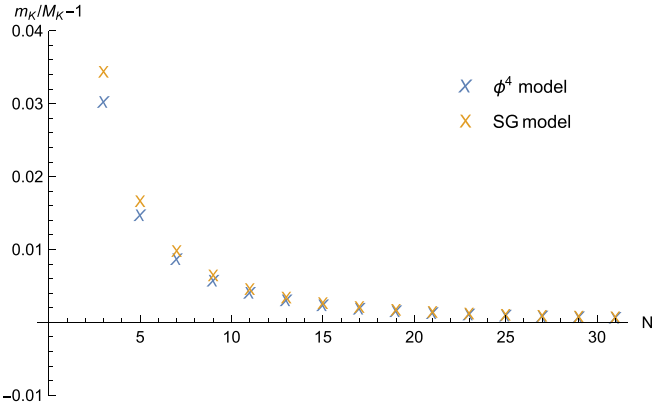

FIG. 5. Relative difference of mechanical kink static energy m_K and field-theoretic value M_K as a function of the number of joints N for the ϕ^4 and SG models.

where

$$\kappa = \frac{1}{v_R - v_L} \int_{v_L}^{v_R} dt\, V(t). \tag{41}$$

The corresponding values for the ϕ^4 model are $R_K = \sqrt{15/2}$ and $m_K = \sqrt{32/15} \approx 1.46$. The latter value is not that far from the field-theoretic value $M_K = 4/3$. However, as we show in Fig. 5, the mass of higher-N mechanical kinks approaches M_K only relatively slowly.

The $N = 1$ mechanical kink has only one massive normal mode: The Derrick mode. This mode is associated with infinitesimal scaling and has been identified as a crucial element in constructing relativistic CCMs for $K\bar{K}$ collisions in various field theories [11]. Its (angular) frequency is universally given as $\omega_D^2 = Q/M$, where Q is the second moment of static energy density. The corresponding formula for the $N = 1$ mechanical field reads $q_M = (v_R - v_L)^2/12R_K$. In the case of the ϕ^4 theory, we have $q_M = \sqrt{5/6} \approx 0.91$, which is quite far from the field-theoretic value $Q \approx 0.43$.

In general, a mechanical kink with $N + 1$ joints has $2N$ normal modes. The lowest one is a zero mode corresponding to the overall translation of joints. The remaining $2N - 1$ modes are massive modes. As $N \to \infty$, we should somehow recover the corresponding spectrum of field-theoretic kinks. This typically consists of a certain number of localized modes and a continuous spectrum of radiation modes, depending on the model at hand.

In Figs. 6 and 7 we show that this correspondence (if it exists at all) is not very visible in the displayed range $N \leqslant 17$. For instance, Fig. 7 hints at some convergence of the third normal modes towards the (blue dashed) line of the ϕ^4 kink's only massive mode, but this could be entirely coincidental and further investigation into higher N is needed to draw any conclusions.

These results illustrate that the correspondence between relatively-high-N non-BPS mechanical kinks and field-theoretic kinks is not as simple, as one might hope, especially regarding the structure of normal modes. Let us now see how the situation differs for static solutions of $L_M^{\rm BPS}$.

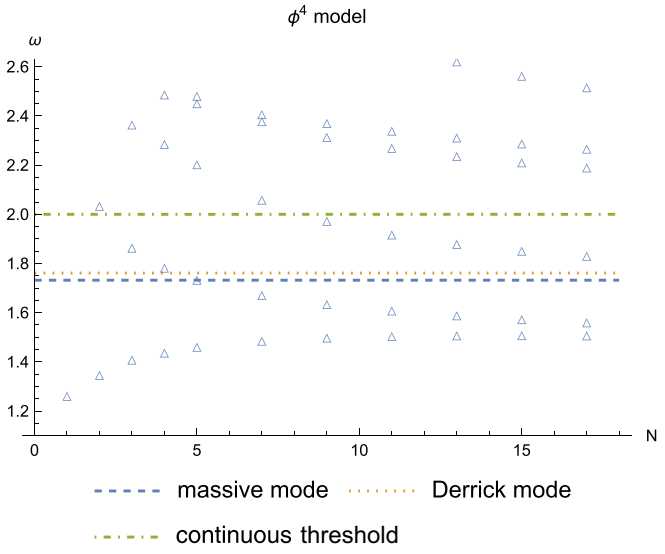

FIG. 6. Distribution of frequencies ω of normal modes as a function of N for the ϕ^4 model. Only a few of the lowest frequencies are displayed and zero modes are omitted.

B. BPS mechanical kinks

In the BPS scheme, the static energy reads

$$E_M^{\rm BPS} = \sum_{a=0}^{N-1} \left[\frac{(\Delta\phi_a)^2}{2\Delta x_a} + \frac{\Delta x_a}{2} \left(\frac{\Delta \mathcal{W}(\phi_a)}{\Delta \phi_a} \right)^2 \right]. \tag{42}$$

Proceeding as in the preceding section, we first eliminate the coordinates of the joints via their equations of motion

$$\Delta x_a = \frac{(\Delta\phi_a)^2}{\Delta \mathcal{W}(\phi_a)}. \tag{43}$$

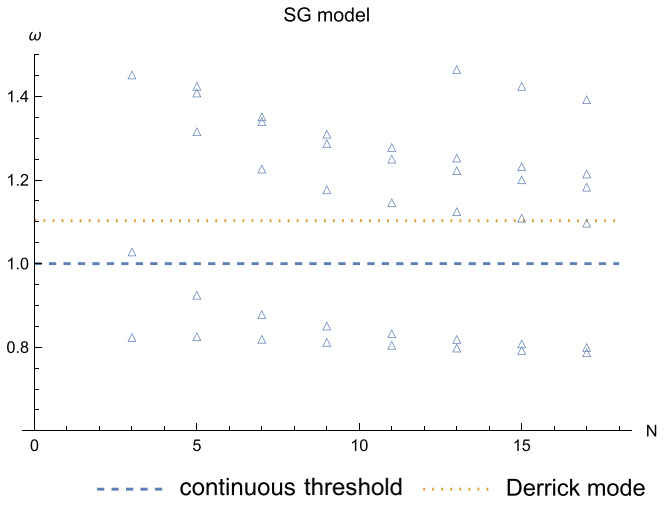

FIG. 7. Distribution of frequencies ω of normal modes as a function of N for the SG model. Only a few of the lowest frequencies are displayed and zero modes are omitted.

In contrast with the non-BPS case, if we insert this relation back into the $E_M^{\rm BPS}$ we obtain a pure number

$$\begin{aligned} E_M^{\rm BPS} &\underset{(43)}{\longrightarrow} \sum_{a=0}^{N-1} \Delta \mathcal{W}(\phi_a) = \mathcal{W}(\phi_N) - \mathcal{W}(\phi_0) \\ &= \mathcal{W}(v_{\rm R}) - \mathcal{W}(v_{\rm L}) \equiv M_K, \end{aligned} \tag{44}$$

which is given by the difference of superpotentials evaluated for vacua at $\pm\infty$, the field-theoretic BPS mass of the kink M_K.

We can establish this result in a standard way by completing the energy in a (sum of) square(s) in the manner of Bogomol'nyi [23]:

$$\begin{aligned} E_M^{\rm BPS} &= \sum_{a=0}^{N-1} \left[\frac{(\Delta\phi_a)^2}{2\Delta x_a} + \frac{\Delta x_a}{2} \left(\frac{\Delta \mathcal{W}(\phi_a)}{\Delta \phi_a} \right)^2 \right] \\ &= \sum_{a=0}^{N-1} \frac{\Delta x_a}{2} \left(\frac{\Delta\phi_a}{\Delta x_a} - \frac{\Delta \mathcal{W}(\phi_a)}{\Delta \phi_a} \right)^2 + \sum_{a=0}^{N-1} \Delta \mathcal{W}(\phi_a) \\ &\geqslant \sum_{a=0}^{N-1} \Delta \mathcal{W}(\phi_a) = M_K. \end{aligned} \tag{45}$$

The minimization of energy is achieved by vanishing the squares, giving us the conditions (43).

Interestingly, BPS mechanical kinks have unconstrained heights of the joints because there is no equivalent of Eq. (39) that would uniquely determine ϕ_a. Indeed, ϕ_a is arbitrary as long as $\Delta x_a > 0$. This amounts to the condition

$$\mathcal{W}(\phi_{a+1}) > \mathcal{W}(\phi_a) \, \forall \, a. \tag{46}$$

For $N = 1$, the only difference from the non-BPS case is in the parameter $\kappa_{\rm BPS}$ [compare with Eq. (41)]:

$$\kappa_{\rm BPS} = \frac{1}{2(v_{\rm R} - v_{\rm L})^2} \left(\int_{v_{\rm L}}^{v_{\rm R}} dt \, W(t) \right)^2. \tag{47}$$

Its value for the ϕ^4 model is $\kappa_{\rm BPS} = 2/9$, giving us $R_K = 3$, $m_K = M_K = 4/3$, and $q_M = 1$.

The structure of normal modes is also very different compared with non-BPS mechanical kinks. A BPS mechanical kink has N zero modes, corresponding to an overall shift in the position of joints and the freedom to make infinitesimal shifts of each ϕ_a. Consequently, it has only N massive normal modes, in contrast with $2N - 1$ massive modes for non-BPS mechanical kinks.

The frequencies of these massive modes, however, do depend on the value of ϕ_a. As an illustration, in Fig. 8 we display the frequencies of the two massive modes of the $N = 2$ BPS mechanical kink as functions of ϕ_1 for the ϕ^4 model. In fact, it is easy to work out explicit formulas:

$$\omega_1 = \frac{\sqrt{4 + 2\phi_1^2}}{\sqrt{3}}, \quad \omega_2 = \frac{1}{3} \sqrt{54\phi_1^2 + \frac{16}{\phi_1^2} - 28}. \tag{48}$$

A salient feature of Fig. 8 is the expected mirror symmetry under $\phi_1 \to -\phi_1$ and the fact that, at the center $\phi_1 = 0$, the second massive mode diverges, i.e., $\omega_2 \to \infty$. This is a footprint of the coordinate degeneracy: At that point the $N = 2$ BPS mechanical kink is indistinguishable from the $N = 1$

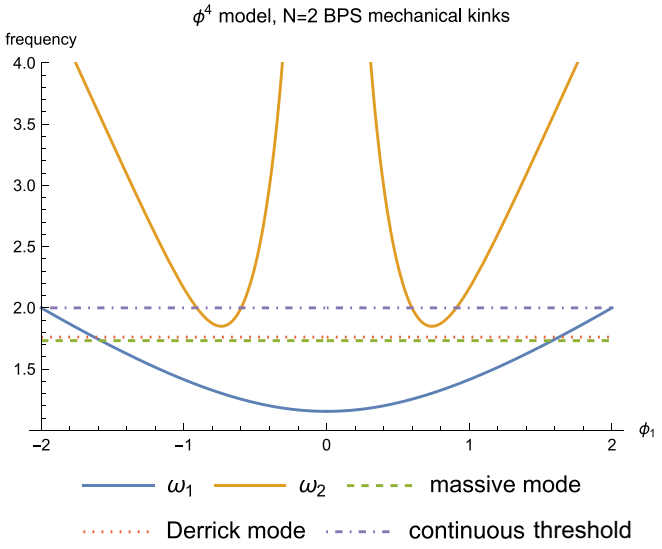

FIG. 8. Dependence of frequency of two massive modes for $N = 2$ BPS mechanical kinks on the height of the middle joint ϕ_1. The horizontal lines indicate relevant frequencies for the field-theoretic kink in the ϕ^4 theory.

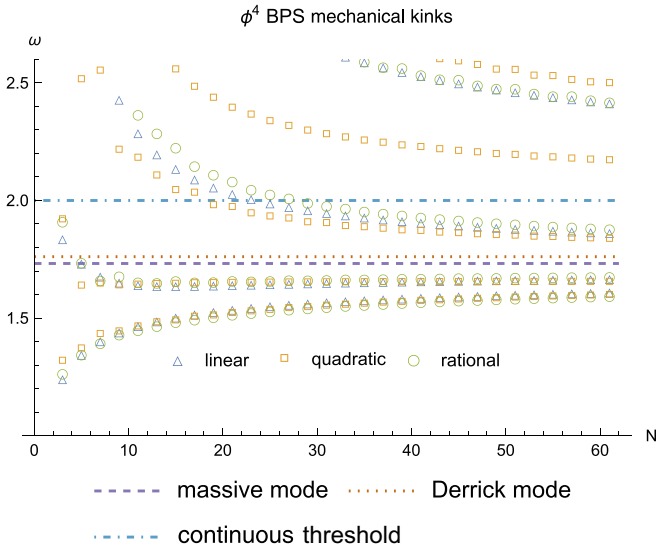

FIG. 9. Frequencies of normal modes for ϕ^4 BPS mechanical kinks as a function of the number of joints $N + 1$. We depict a gradual approach of the values for three different value assignments of field values ϕ_a as described in the text.

mechanical kink. Indeed, the value $\omega_1(\phi_1 = 0) = 2/\sqrt{3}$ is the same as the $N = 1$ Derrick mode. What is more surprising is the fact that the lengths of segments

$$\Delta x_0 = \frac{3}{2 - \phi_1}, \quad \Delta x_1 = \frac{3}{2 + \phi_1} \tag{49}$$

are both positive in the range $\phi_1 \in (-2, 2)$. Thus, the middle joint can also be placed outside $[-1, 1]$, contrary to expectations.

Finally, let us address the question of recovering the spectrum of normal modes of the ϕ^4 kink in the limit $N \to \infty$. Compared with non-BPS mechanical kinks, the situation is complicated by the fact that N massive normal modes depend on $N - 1$ free parameters, the ϕ_a.

To make progress, we studied several somewhat random types of value assignments for the heights of joints, referred to as linear, quadratic, and rational, given by the formulas

$$\phi_a = -1 + \frac{2a}{N} \quad \text{(linear)}, \tag{50}$$

$$\phi_a = -1 + \frac{1}{2}\left(\frac{2a}{N}\right)^2 \quad \text{(quadratic)}, \tag{51}$$

$$\phi_a = 1 - \frac{2(N - a)}{a + N} \quad \text{(rational)}. \tag{52}$$

In Fig. 9 we display how the lowest-lying frequencies of normal modes change with increasing N for all three types of assignments. We see that, especially for the two lowest massive modes, the frequencies tend to converge to the same values for all three assignments. This hints that the same limiting spectrum should be reached for any choice of ϕ_a. However, as was the case for non-BPS mechanical kinks, the convergence to $\sqrt{3}$, the frequency of the ϕ^4 kink's shape mode, is very slow, if it exists at all. All that we can claim is that the convergence towards the shape mode is very slow in the displayed range $N \leqslant 61$.

Another crucial property of BPS mechanical kinks is the existence of N zero modes due to the degeneracy of the solution. For example, the $N = 2$ mechanical kink has not only translational zero mode but also a zero mode corresponding to an infinitesimal change of ϕ_1, the height of the middle joint. This extra zero mode has an interesting and counterintuitive impact on the dynamic of $N = 2$ mechanical kinks. We can easily imagine (and we observe it in numerical simulations) that during dynamical evolution, the coordinate ϕ_1 drifts from its initial value, as its change does not cost any energy. We observe that once the middle joint becomes very close to one of the outer joints, the latter quickly accelerate to infinity. In this way, the $N = 2$ mechanical kink sheds one of its outer joints and becomes effectively an $N = 1$ mechanical kink. This phenomenon is called joint ejection and we reported it in our previous paper [22].

Although the joint ejections were observed for sufficiently perturbed $N \geqslant 2$ non-BPS mechanical kinks, in the BPS case they are practically inevitable due to the presence of extra zero modes. This leaves only the $N = 1$ mechanical kink as a truly stable solution in BPS mechanization.

IV. SCATTERING OF MECHANICAL KINKS

In this section we investigate the simplest forms of scattering between mechanical kinks to showcase the second conceptual advancement of this paper, what we call a loose order mechanization. As we will see, the analysis of mechanical-$K\bar{K}$ scattering requires including noncanonical orderings of the joints and construction of an effective Lagrangian that incorporates these different orderings. We also present numerical results for the dynamics of a symmetric $N = 3$ mechanical field and we find qualitatively similar

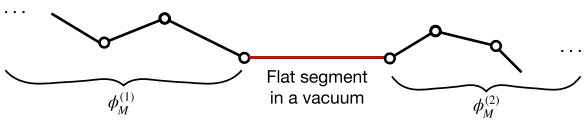

FIG. 10. Illustration of the decoupling property. If the mechanical field consists of two parts connected by a flat segment in a vacuum, the coordinates in the left and right parts of the mechanical field do not interact.

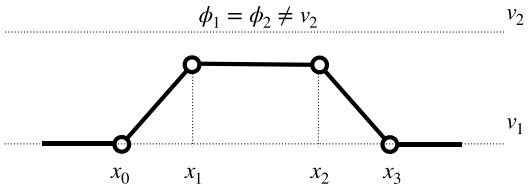

FIG. 11. The $N = 3$ symmetric mechanical field.

behavior to field theory, namely, that the mechanical-$K\bar{K}$ pair undergoes bounces or forms (mechanical) bions. We analyze the scattering of both non-BPS and BPS mechanical kinks and comment on the differences.

A. Decoupling

The compact nature of mechanical fields, i.e., that they have finite extents outside of which there are only exact vacua, allows us to superpose objects, e.g., mechanical kinks or mechanical oscillons, without introducing any interaction between them. This is most easily visible at the effective Lagrangian level. Taking a generic mechanical field and fixing the ath segment to a vacuum, say, $\phi_a = \phi_{a+1} = v$, while keeping x_a and x_{a+1} dynamical, it is easy to see that the effective Lagrangian consists of two decoupled pieces:

$$L_M[\phi_M] \xrightarrow[\phi_a,\phi_{a+1}\to v]{} L_M\big[\phi_M^{(1)}\big] + L_M\big[\phi_M^{(2)}\big]. \tag{53}$$

In other words, there remain no interacting terms that could inform the constituent mechanical fields $\phi_M^{(1,2)}$ about each other's existence.[5] Thus, the two parts evolve according to their respective dynamics as if the other piece is not there at all (see Fig. 10). This is of course true only until they start to overlap, where the very description of the dynamics via effective Lagrangians (27) or (28) is invalid.

As a consequence, a mechanical kink and an anti-mechanical-kink separated by a vacuum segment of arbitrary length do not impart any force on one another. This should be compared with what is going on in field theory, where a well-separated $K\bar{K}$ configuration experiences an exponentially damped attractive force, precisely because field-theoretic solitons are not compact.[6] This presents somewhat of a roadblock to naive investigations of mechanical-$K\bar{K}$ scattering. Indeed, the dynamics derived from the effective Lagrangian (27) is trivial before the collision (no force) and undefined for the moment of contact as $L[\{x_a, \phi_a\}]$ applies only for canonically ordered mechanical fields.

One way around this obstacle is to investigate approximate mechanical kinks. As an example, we can consider a symmetric $N = 3$ mechanical field depicted in Fig. 11 with a middle segment not exactly in a vacuum but arbitrarily close to it.

However, the excess energy in the central segment would manifest as a constant attractive force between the (approximate) mechanical kinks. Importantly, this force would be long range and clearly an artifact of the selected configuration. In fact, we should not see the mechanical field in Fig. 11 as describing well-separated mechanical kinks; the presence of a long-range force between them makes them manifestly not well separated. Rather, we should say that Fig. 11 depicts a symmetric mechanical oscillon and has (*a priori*) nothing to do with mechanical-$K\bar{K}$ dynamics.

Even for more elaborate mechanical fields, long-range forces would remain present simply because piecewise linear functions cannot rapidly approximate a constant (without actually being identical to it), unlike the exponentially decaying tails of kinks in the field theory. In this way, the investigation of approximate mechanical-$K\bar{K}$ scattering is irreparably contaminated by unphysical long-range forces.

Fortunately, we can investigate scattering of mechanical kinks directly and in a natural way, as we do in this section.

B. Rigid $K\bar{K}$ scattering

Let us consider a superposition of a mechanical kink and anti-mechanical-kink with widths R_K separated by a flat middle segment of length R in a vacuum v_2. Specifically,

$$\begin{aligned}\phi_M^{K\bar{K}} &= v_1\theta(-x - R_K - R/2) + [\theta(x + R_K + R/2) \\ &\quad - \theta(x + R/2)]\left(\frac{v_2 - v_1}{R_K}(x + R_K + R/2) + v_1\right) \\ &\quad + v_2[\theta(x + R/2) - \theta(x - R/2)] \\ &\quad + [\theta(x - R/2) - \theta(x - R_K - R/2)] \\ &\quad \times \left(-\frac{v_2 - v_1}{R_K}(x - R/2) + v_2\right) \\ &\quad + v_1\theta(x - R/2 - R_K).\end{aligned} \tag{54}$$

Note that $\phi_M^{K\bar{K}} = \phi_M^K(x + R/2) + \phi_M^{\bar{K}}(x - R/2) + v_1$, where ϕ_M^K and $\phi_M^{\bar{K}}$ are an $N = 1$ mechanical kink and an $N = 1$ anti-mechanical-kink, respectively.

The key to analyze the dynamics of $\phi_M^{K\bar{K}}$ is to realize that there are four distinct orderings of joints (or stages; see Fig. 12) depending on the value of R, each of which is governed by a different effective Lagrangian. Each stage follows from the previous one by continuation of R to more negative values. In turn, R has a different meaning in each stage. When $R > 0$, it is the distance between a mechanical kink and an

[5]During dynamical evolution, a mechanical field can pass through a decoupled configuration. In such a case, however, nonzero derivatives preserve the interaction between the two parts, so the decoupling does not occur.

[6]In special field theories, however, compact solutions can be present [24–27]. Their behavior is quite similar to the mechanical kinks and mechanical oscillons presented here (or, more correctly, vice versa).

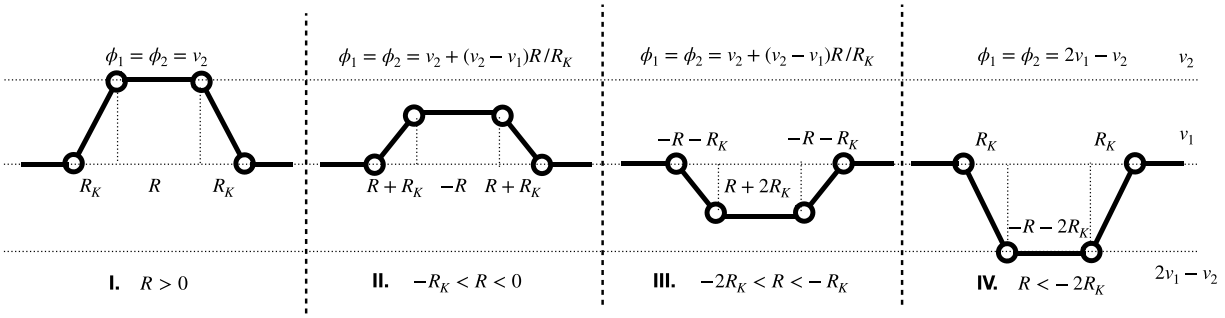

FIG. 12. Various stages of the $N = 3$ mechanical field depending on the value of R. If $R > 0$, the configuration is a mechanical kink and antikink interpolating vacua v_1 and v_2 separated by distance R. The width $R_K > 0$ is assumed to be always positive. In the second and third stages, when $-2R_K < R < 0$, the mechanical field becomes an $N = 3$ mechanical oscillon, first above and then below the vacuum v_1. Its amplitude depends on R in a designated way. In the final stage $R < -2R_K$, the mechanical field can be arbitrarily wide, but since the middle segment does not lie in either vacua (assuming $2v_1 - v_2$ is not another vacuum), it is energetically unfavored.

antikink. When $-R_K < R < 0$, it controls both the height and width of a symmetric $N = 3$ mechanical oscillon that is placed above vacuum v_1, while when $-2R_K < R < -R_K$, R serves a similar role for the mechanical oscillon placed under v_1. Finally, when $R < -2R_K$, the mechanical field $\phi_M^{K\bar{K}}$ resembles an arbitrarily separated anti-mechanical-kink and mechanical kink that interpolate between the values v_2 and $2v_1 - v_2$. If the latter value is not a vacuum of the given model, there is a constant attractive force and the whole configuration is energetically disfavored.

For simplicity, in this section we investigate rigid mechanical-$K\bar{K}$ scattering, where only R is dynamical while R_K is fixed to an appropriate initial value. For the first stage, i.e., assuming $R > 0$, we have

$$L_{\rm I} = \frac{(v_2 - v_1)^2}{4R_K}\dot{R}^2 - \frac{(v_2 - v_1)^2}{R_K} - 2\kappa R_K, \tag{55}$$

where κ is given either as in Eq. (41) for non-BPS mechanization or as in Eq. (47) in the BPS case. Up to an irrelevant constant, $L_{\rm I}$ describes a free particle (with position $R/2$) of mass $2(v_2 - v_1)^2/R_K$.[7] In this stage, the mechanical kinks indeed behave as free particles.

In the second stage, i.e., for $-R_K < R < 0$, we obtain

$$L_{\rm II} = \frac{(v_2 - v_1)^2}{4R_k^2}(R_K - R)\dot{R}^2 - U_{\rm II}, \tag{56}$$

where the potentials for both non-BPS and BPS mechanization read

$$U_{\rm II} = \frac{2R_K}{v_2 - v_1}\left[\mathcal{V}\left(v_2 + \frac{v_2 - v_1}{R_K}R\right) - \mathcal{V}(v_1)\right] - RV\left(v_2 + \frac{v_2 - v_1}{R_K}R\right) - \frac{(v_2 - v_1)^2(R + R_K)}{R_K^2}, \tag{57}$$

$$U_{\rm II}^{\rm BPS} = \frac{R_K^2/(v_2 - v_1)^2}{(R_K + R)}\left[\mathcal{W}\left(v_2 + \frac{v_2 - v_1}{R_K}R\right) - \mathcal{W}(v_1)\right]^2 - \frac{R}{2}W^2\left(v_2 + \frac{v_2 - v_1}{R_K}R\right) - \frac{(v_2 - v_1)^2(R + R_K)}{R_K^2}. \tag{58}$$

It is easy to check that $L_{\rm I} = L_{\rm II}$ at $R = 0$, namely, that the transition from the first stage to the second stage is continuous. This is a direct consequence of continuity of the mechanical field $\phi_M^{K\bar{K}}$ (54).

The Lagrangian $L_{\rm II}$ describes a rigid and symmetric $N = 3$ mechanical oscillon. Its solutions are periodic. Also note that the metric $(v_2 - v_1)^2(R_K - R)/2R_K^2$ is regular at both transitions from the first stage to the second ($R = 0$) and from the second stage to the third at $R = -R_K$. This is also true for the potential which goes to zero at $R = -R_K$. Thus, there are no singularities that prevent us from continuing the variable R below $-R_K$.

The third stage also depicts a rigid $N = 3$ mechanical oscillon which is placed below the vacuum v_1,

$$L_{\rm III} = \frac{(v_2 - v_1)^2}{4R_k^2}(3R_K + R)\dot{R}^2 - U_{\rm III}, \tag{59}$$

where

$$U_{\rm III} = -\frac{2R_K}{v_2 - v_1}\left[\mathcal{V}\left(v_2 + \frac{v_2 - v_1}{R_K}R\right) - \mathcal{V}(v_1)\right] + (2R_K + R)V\left(v_2 + \frac{v_2 - v_1}{R_K}R\right) + \frac{(v_2 - v_1)^2(R + R_K)}{R_K^2}, \tag{60}$$

$$U_{\rm III}^{\rm BPS} = -\frac{R_K^2/(v_2 - v_1)^2}{(R_K + R)}\left[\mathcal{W}\left(v_2 + \frac{v_2 - v_1}{R_K}R\right) - \mathcal{W}(v_1)\right]^2 + \frac{2R_K + R}{2}W^2\left(v_2 + \frac{v_2 - v_1}{R_K}R\right) + \frac{(v_2 - v_1)^2(R + R_K)}{R_K^2}. \tag{61}$$

[7]If we replace R_K with an appropriate static value this would be equivalent to twice the mass of the $N = 1$ mechanical kink.

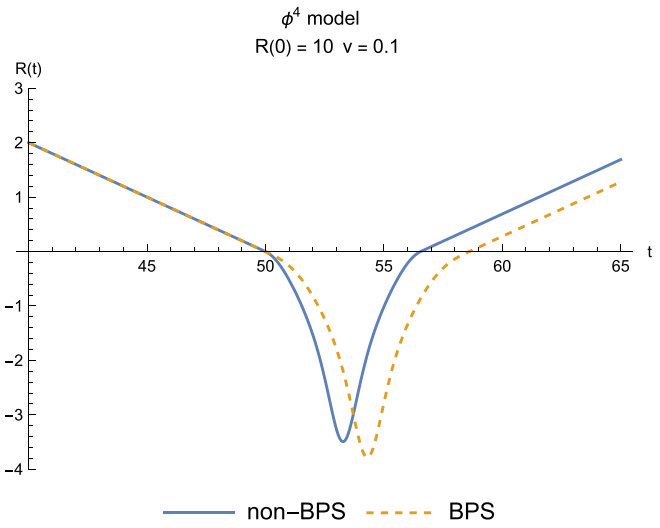

FIG. 13. Example of a rigid mechanical-$K\bar{K}$ collision in the ϕ^4 model. The initial data are $R(0) = 10$ and $\dot{R}(0) \equiv -2v = -0.2$.

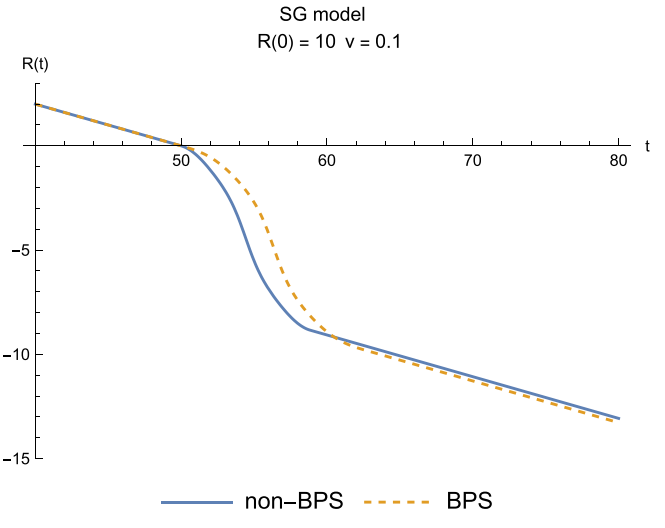

FIG. 14. Example of a rigid mechanical-$K\bar{K}$ collision in the SG model. The initial data are $R(0) = 10$ and $\dot{R}(0) \equiv -2v = -0.2$.

Again, it is easy to check that $L_{\rm II} = L_{\rm III}$ at $R = -R_K$. Furthermore, both the kinetic term and the potential term remain well defined at $R = -2R_K$; thus we may continue to the fourth stage

$$L_{\rm IV} = \frac{(v_2 - v_1)^2}{4R_K}\dot{R}^2 - \frac{(v_2 - v_1)^2}{R_K} - 2\kappa_{\rm IV}R_K, \tag{62}$$

where

$$\kappa_{\rm IV} = \frac{\mathcal{V}(v_1) - \mathcal{V}(2v_1 - v_2)}{v_2 - v_1} - \left(1 + \frac{R}{2R_K}\right)V(2v_1 - v_2), \tag{63}$$

$$\kappa_{\rm IV}^{\rm BPS} = \frac{1}{2}\left(\frac{\mathcal{W}(v_1) - \mathcal{W}(2v_1 - v_2)}{v_2 - v_1}\right)^2 - \frac{1}{2}\left(1 + \frac{R}{2R_K}\right)W^2(2v_1 - v_2). \tag{64}$$

The $L_{\rm IV}$ generically describes a particle in a linearly attractive potential, unless $2v_1 - v_2$ is also a vacuum of the model.

Since all transitions from one stage to the next are continuous, we may collect the fixed-order Lagrangians into a single LOM that captures the dynamics of rigid mechanical-$K\bar{K}$ collisions for the entire range $R \in (-\infty, \infty)$,

$$\begin{aligned} L_{\rm LOM}^{\rm rigid} = {} & L_{\rm I}\theta(R) + L_{\rm II}\theta(-R)\theta(R + R_K) \\ & + L_{\rm III}\theta(-R - R_K)\theta(R + 2R_K) \\ & + L_{\rm IV}\theta(-R - 2R_K), \end{aligned} \tag{65}$$

where $L_{\rm I,II,III,IV}$ are fixed-order Lagrangians given above. Note that $L_{\rm LOM}^{\rm rigid}$ is a continuous function of R. Furthermore, $L_{\rm LOM}^{\rm rigid}$ is nothing but a direct integration of the mechanical field $\phi_M^{K\bar{K}}$ assuming $R_K = {\rm const} > 0$, i.e.,

$$L_{\rm LOM}^{\rm rigid} = \int_{-\infty}^{\infty} dx\, \mathcal{L}\big(\phi_M^{K\bar{K}}\big), \tag{66}$$

allowing for all possible orderings of joints.

As there are no modes through which (rigid) mechanical kinks can lose energy, they either are bound to reflect off each other (in the case of, say, the ϕ^4 model) or go through each other (in the case of, e.g., the SG model), as illustrated in Figs. 13 and 14.

Let us further point out that there is a direct field-theoretic analog of $L_{\rm rigid}$ based on the *Ansatz*

$$\phi = \phi_K[x + R(t)/2] + \phi_{\bar{K}}[x - R(t)/2] + v_1, \tag{67}$$

where ϕ_K is the single-soliton solution for the given model. The corresponding effective Lagrangian does the same job as $L_{\rm rigid}$ of Eq. (65). However, there are conceptual differences. In field theory, one must be careful about placing the kinks sufficiently apart. This is especially true for the ϕ^8 model where the kinks have long polynomial tails and a naive superposition *Ansatz* like (67) is not suitable for numerical investigation [27]. In contrast, the mechanical-$K\bar{K}$ superposition *is* an exact solution of the equations of motion for any $R > 0$. Thus the outcome of the collision is automatically independent of the initial separation. We can summarize this by saying that the short-range interactions of field theory are replaced by contact interactions in mechanization.

C. Mechanical-$K\bar{K}$ scattering

Let us now turn to $R_K(t)$. The mechanical kinks now possess a Derrick mode that allows the resonant transfer of kinetic energy, which manifests as bouncing, which is when a mechanical-$K\bar{K}$ pair temporarily reemerges from the second stage into the first stage but does not have sufficient kinetic energy to fly apart and instead plunges again below the $R = 0$ line. Note that this gives us an operational definition of the number of bounces as the number of zeros of $R(t)$ divided by 2 minus 1.[8]

[8]This is irrespective of what the outcome of the scattering is.

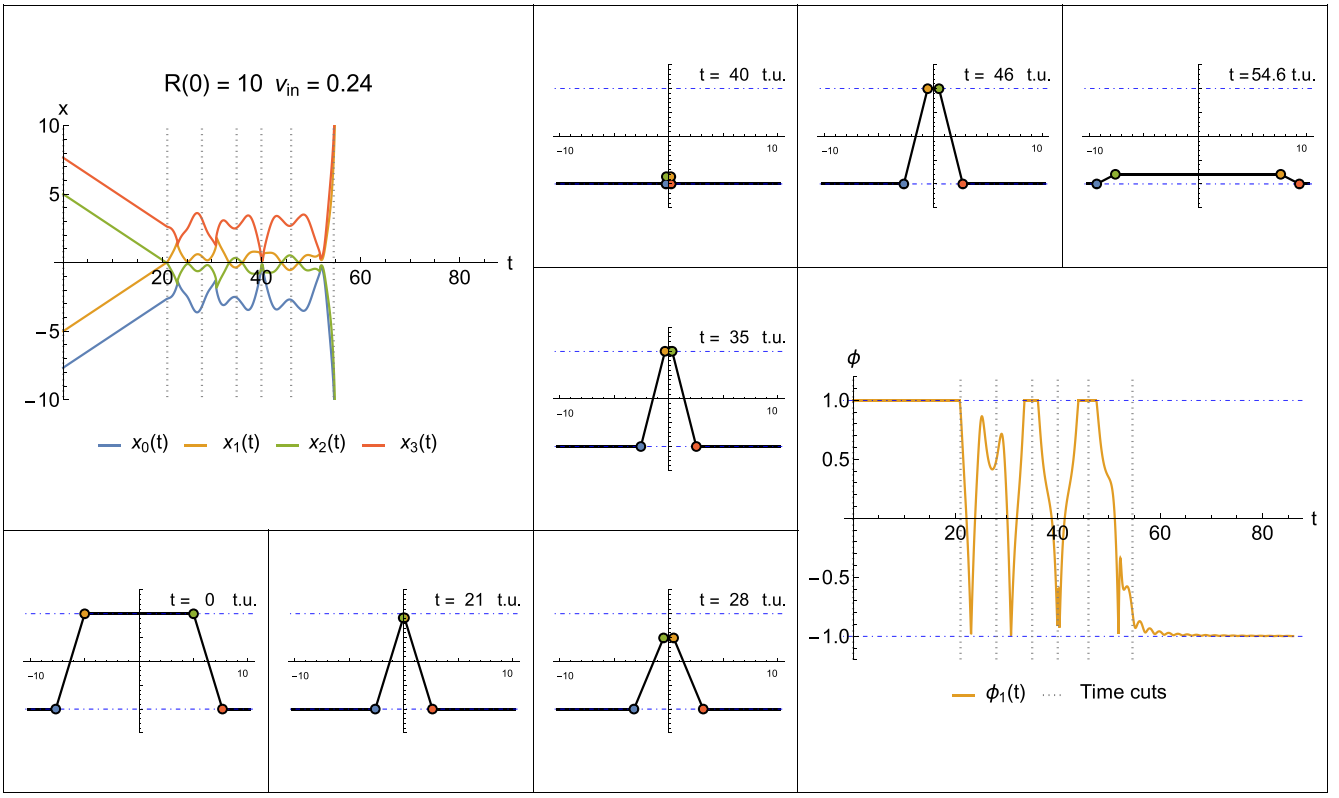

FIG. 15. Collision of the mechanical-$K\bar{K}$ pair in the ϕ^4 model (non-BPS). The initial data are $R(0) = 0$, $\dot{R}(0) \equiv -2v_{\rm in} = -0.48$, $R_K(0) = \sqrt{15(1-v_{\rm in}^2)/2}$, and $\dot{R}_K(0) = 0$. Here we see a formation of a short-duration mechanical oscillon. There are two bounces (around $t = 35$ and 46) after which the mechanical oscillon rapidly decays into the -1 vacuum.

With dynamical $R_K(t)$, the $N = 3$ mechanical oscillon in the second stage can decay, i.e., its width grows exponentially with time, while the height exponentially decreases (see [22] for details). Hence, nonrigid mechanical kinks display more complicated behavior with two primary outcomes: A well-separated mechanical-$K\bar{K}$ pair with excited Derrick modes or a state of a decayed mechanical oscillon. The first stage is given as

$$L_{\rm I}^{K\bar{K}} = \frac{1}{2} g^{\rm I}_{ab} \dot{X}_a \dot{X}_b - \frac{(v_2 - v_1)^2}{R_K} - 2\kappa R_K, \tag{68}$$

where $X_a = \{R, R_K\}$ and the metric reads

$$g^{\rm I} = \frac{2}{3R_K} \begin{pmatrix} 3 & 3 \\ 3 & 4 \end{pmatrix}. \tag{69}$$

There are no singularities in either metric or potential along the R coordinate. The second stage is described by

$$L_{\rm II}^{K\bar{K}} = \tfrac{1}{2} g^{\rm II}_{ab} \dot{X}_a \dot{X}_b - U_{\rm II}, \tag{70}$$

where $U_{\rm II}$ is the same as in the preceding section and the metric reads

$$g^{\rm II} = \frac{1}{3R_K^4} \begin{pmatrix} 6R_K^2(R_K - R) & 6R_K\left(R_K^2 + R^2\right) \\ 6R_K\left(R_K^2 + R^2\right) & -4\left(R^3 - 2R_K^3\right) \end{pmatrix}. \tag{71}$$

From the formulas for the determinant and Ricci scalar

$$|g^{\rm II}| = -\frac{4(R_K + R)\left(R^2 R_K + 5RR_K^2 - R_K^3 + R^3\right)}{3R_K^6}, \tag{72}$$

$$\mathcal{R} = \frac{9R_K^4\left(R^2 R_K - 2RR_K^2 - R_K^3 + R^3\right)}{2(R_K + R)^2\left(R^2 R_K + 5RR_K^2 - R_K^3 + R^3\right)^2} \tag{73}$$

we see that there is a physical singularity at the transition into the third stage, i.e., at $R = -R_K$. Unlike in the rigid case, we are now unable to continue to more negative values; the mechanical field cannot attain values below the vacuum v_1. This is an unphysical artifact that can be traced to the so-called null-vector problem, in which the metric is degenerate at $R = -R_K$.

Hence, the full effective Lagrangian for mechanical-$K\bar{K}$ scattering has only two stages:

$$L_{\rm LOM}^{K\bar{K}} = L_{\rm I}\theta(R) + L_{\rm II}\theta(-R). \tag{74}$$

A CCM that has similar characteristics to $L_{\rm LOM}^{K\bar{K}}$ is given by the *Ansatz*

$$\phi = \phi_K[b(t)[x + a(t)]] + \phi_{\bar{K}}\{b(t)[x - a(t)]\} + v_1. \tag{75}$$

The corresponding effective Lagrangian is described in [11] and suffers from the same null vector (or flatness) problem, namely, that the metric has a singularity at $a = 0$. There are also known remedies for this malady, either by choosing a different moduli space with massive modes supplanted into

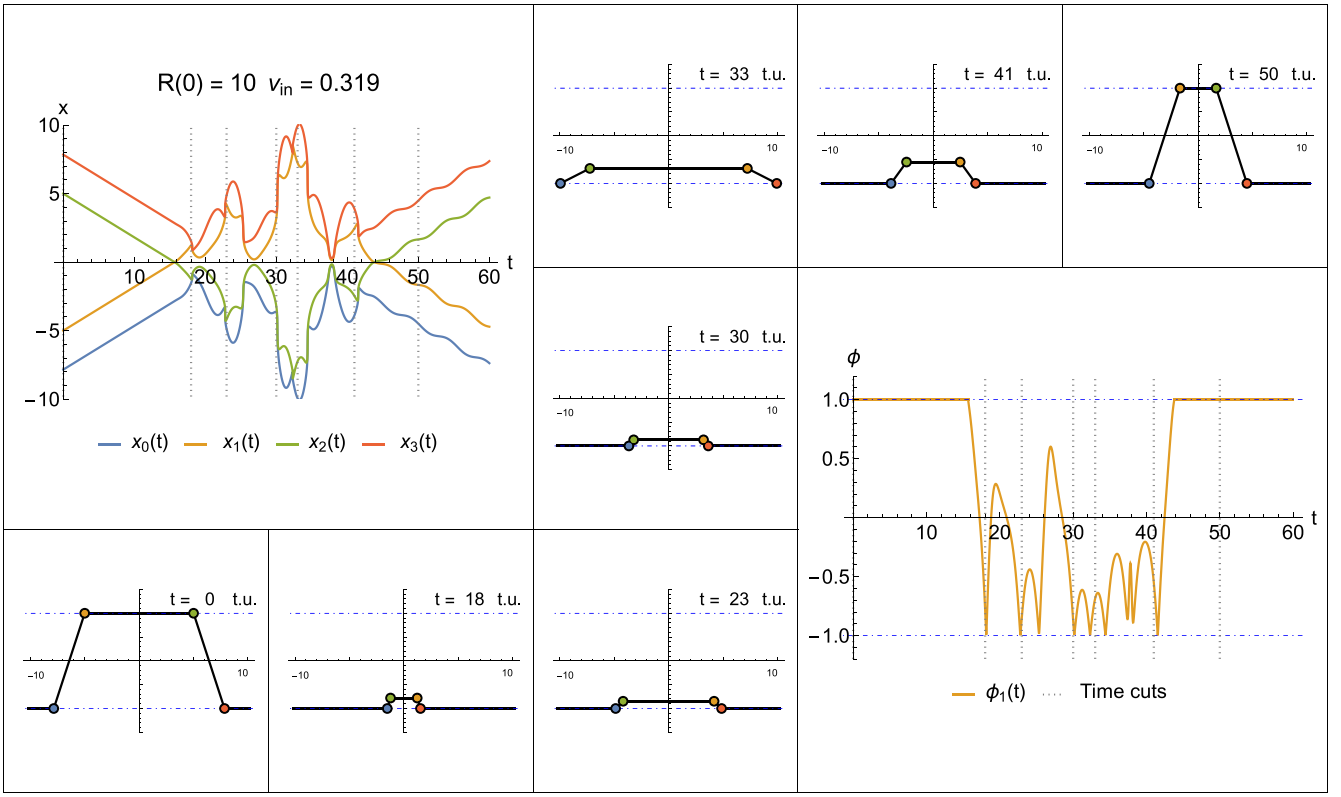

FIG. 16. Collision of mechanical-$K\bar{K}$ pairs in the ϕ^4 model (BPS). The initial data are $R(0) = 0$, $\dot{R}(0) \equiv -2v_{\text{in}} = -0.638$, $R_K(0) = 3\sqrt{(1 - v_{\text{in}}^2)}$, and $\dot{R}_K(0) = 0$. Here the mechanical oscillon is formed for roughly 25 t.u. and disintegrates into a excited mechanical-$K\bar{K}$ pair.

the above *Ansatz* with judiciously chosen amplitude moduli (see [10]) or by including the Derrick modes in a perturbative fashion as done in [11].

The flatness problem present in $L_{\text{LOM}}^{K\bar{K}}$ is a consequence of too simple a mechanical field. Indeed, from the formula (54) we see that at $R = -R_K$ the mechanical field becomes an exact vacuum everywhere, i.e., $\phi_M^{K\bar{K}} = v_1$. Moreover, at this point $\partial_R \phi_M^{K\bar{K}} = -\partial_{R_K} \phi_M^{K\bar{K}}$.

The null-vector problem, however, should all but disappear for higher-N mechanical fields, where there are more degrees of freedom and it is easy to avoid $\phi_M = v_1$ for all values of R. Investigation of higher-N mechanical-$K\bar{K}$ collisions is left for future work. We display typical mechanical-$K\bar{K}$ scattering in Figs. 15–17.

In Fig. 18 we display the time dependence of the center value of the mechanical field $\phi_M(x = 0)$ for a range of initial velocities in the ϕ^4 model. The dark blue color represents the $+1$ vacuum, while the white color stands for the -1 vacuum. A bouncing occurs for such velocities when the value of $\phi_M(x = 0)$ eventually returns to $+1$; these are the dark blue columns indicating that the mechanical-$K\bar{K}$ pair has been reformed after the initial collision. On the other hand, the white columns correspond to situations where the mechanical oscillon decayed to the -1 vacuum. The reader should compare Fig. 18 with Fig. 1.

Let us make several comments.

First, there exists a critical velocity above which the mechanical-$K\bar{K}$ pair scatters elastically. The corresponding value for $K\bar{K}$ collisions in the ϕ^4 theory is $v_{\text{crit}} = 0.2598$ [11], while for non-BSP mechanization $L_{\text{LOM}}^{K\bar{K}}$ it is around 0.32 (upper half of Fig. 18) and around 0.44 for the BPS case (lower half of Fig. 18). It is curious that the BPS mechanization nature makes the match with the field theory in this regard worse.

Second, there also exists a minimal velocity below which bouncing does not occur. This is especially visible for BPS mechanization, where $v_{\text{min}} \approx 0.28$ and below which there is a clear change in character of the collisions. For the non-BPS version (the upper part of Fig. 18), it is much harder to ascertain the value of v_{min} without a careful search. Certainly, there does not seem to be a qualitative change of the mechanical-$K\bar{K}$ scattering like in the BPS case. In this regard, the BPS case is more similar to the field theory.

The third aspect, and perhaps the most striking, is the absence of smooth edges between bouncing windows and bion chimneys in both non-BPS and BPS cases. In field theory, bouncing windows begin and end at practically vanishing values of outgoing velocities so that the transitions to bion chimneys are continuous. In our case, however, bouncing windows start and end abruptly at finite velocities. Currently, we cannot give a reason why this is so or what the significance of this phenomenon is. We suspect it is a clue that could lead to further conceptual improvements of the mechanization, but the investigation of these aspects of mechanical-$K\bar{K}$ scattering are beyond the scope of the present work.

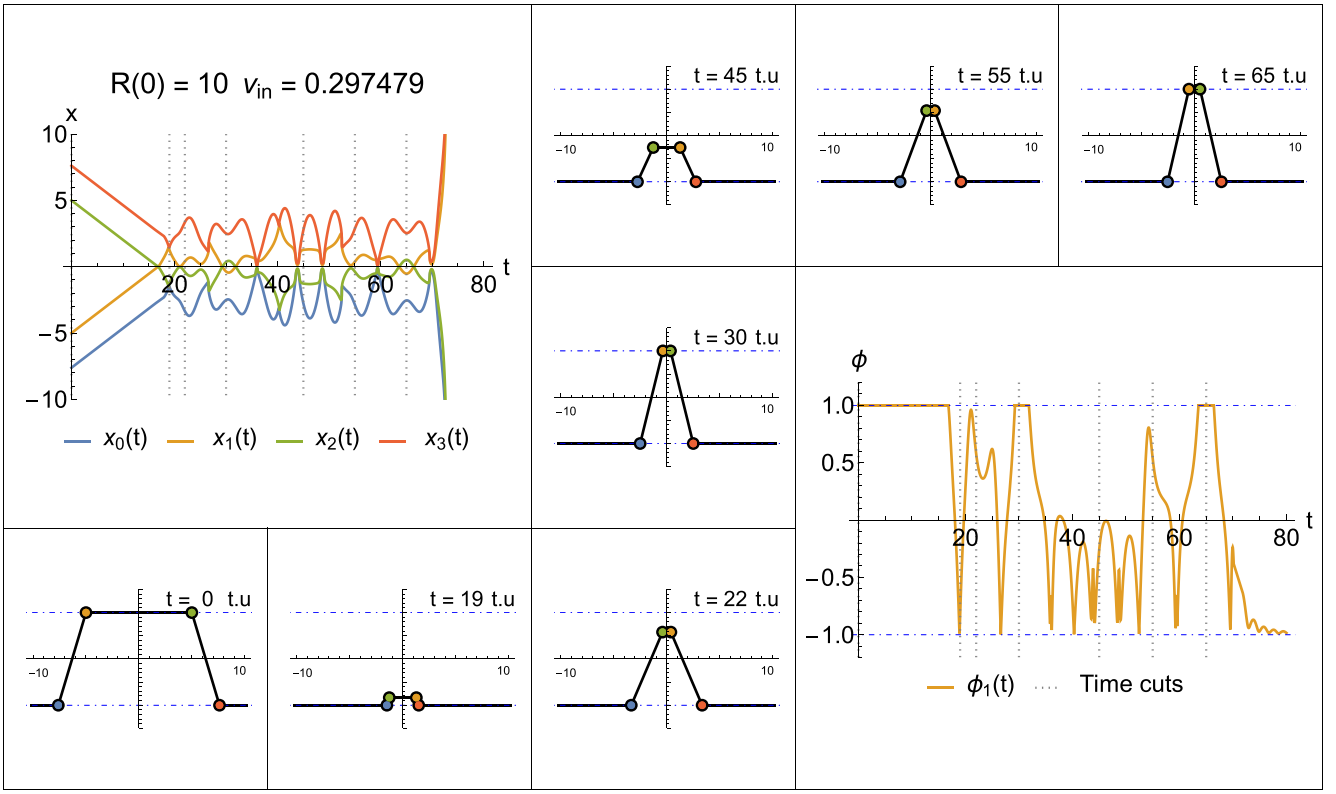

FIG. 17. Collision of mechanical-$K\bar{K}$ pairs in the ϕ^4 model (non-BPS). The initial data are $R(0) = 0$, $\dot{R}(0) \equiv -2v_{\text{in}} = -0.594958$, $R_K(0) = \sqrt{15(1 - v_{\text{in}}^2)}/2$, and $\dot{R}_K(0) = 0$. Here we see two bounces (around $t = 22$ and 65) after which the pair flies apart to infinity.

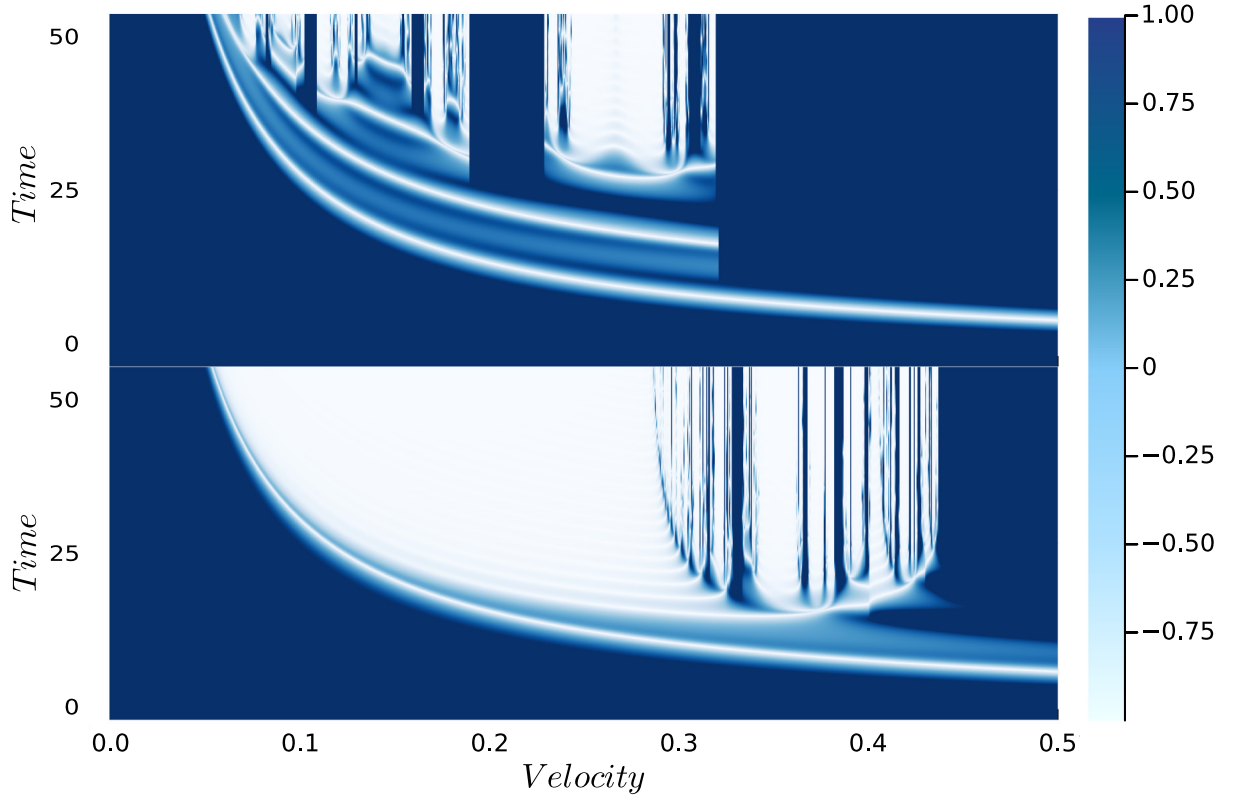

FIG. 18. Dependence of the center value $\phi_M(x = 0)$ on time for a range of initial velocities in the ϕ^4 model. The initial separation of the mechanical-$K\bar{K}$ pair is set to $R(0) = 5$. The upper part shows non-BPS mechanization and the lower part BPS mechanization.

D. LOM

We can generalize the concept of LOM as follows. Given a mechanical field ϕ_M with joints placed at positions $\{x_0, \ldots, x_N\}$, the effective Lagrangian describing its dynamics is given by

$$L_{\rm LOM} = \sum_{\sigma \in P_{N+1}} L_{\rm M}\big(\{x_\sigma, \phi_\sigma^{\rm true}\}\big) \prod_{a=0}^{N-1} \theta(x_{\sigma(a+1)} - x_{\sigma(a)}), \quad (76)$$

where P_{N+1} is the set of all permutations of $N+1$ indices and $L_M(\{x, \phi\})$ is a fixed order effective Lagrangian given by the formula (27). Note that the (true) heights of the joints $\phi^{\rm true}$ depend on the given permutation of joints (e.g., in Fig. 12 we see that the heights of joints have different values in each stage). Depending on which $L_M(\{x, \phi\})$ is taken, either non-BPS or BPS, the resulting LOM would describe either non-BPS or BPS dynamics.

Let us stress that $L_{\rm LOM}$ is simply a result of direct integration of the Lagrangian density, i.e.,

$$L_{\rm LOM} = \int_{-\infty}^{\infty} dx\, \mathcal{L}(\phi_M), \quad (77)$$

allowing $\{x_0, \ldots, x_N\}$ to take all possible values. Consequently, the chain of Heaviside functions in the formula (76) is there to enforce that the appropriate fixed-order Lagrangian is switched on.

Finally, let us comment that a generic mechanical field for which all $2N$ degrees of freedom are dynamical is not going to be directly extendable beyond canonical orderings of joints. This is due to the presence of singularities in the moduli space that we discussed in Sec. II [see, e.g., (24)]. Generically, the ϕ_a need to be constrained in an appropriate way to ensure the continuity of the mechanical field at each contact $\Delta x_a = 0$.

V. SUMMARY AND OUTLOOK

In this paper we have introduced two conceptual advancements of mechanization compared with [22]. First is the BPS mechanization that replicates the BPS nature of kinks in field theory. Unlike the non-BPS mechanical kinks with static energies m_K approaching the field-theoretic mass M_K only very slowly, as evident from Fig. 5, the BPS mechanical kinks saturate the same bound $m_K = M_K$ for all N. There is also a major difference in the number of zero modes. Non-BPS mechanical kinks have $2N-1$ massive normal modes and only one zero mode associated with translational symmetry. On the other hand, BPS mechanical kinks have N massive modes and $N-1$ additional zero modes that stem from the arbitrariness of the heights of joints ϕ_a. These extra zero modes make the $N > 1$ BPS mechanical kinks dynamically unstable. We observed that they are very prone to joint ejections, a boundary joint flying off to infinity, effectively reducing the number of degrees of freedom. The joint ejections happen also for non-BPS mechanical kinks, but in that case there is an energy barrier to overcome. In contrast, in the BPS case the joint ejections may be triggered by the slightest perturbation. Thus, we are led to the conclusion that only the $N = 1$ BPS mechanical kink is a dynamically stable solution.

We have also illustrated the convergence (or lack thereof) of the distribution of normal modes to the spectrum for kinks in Figs. 6–9. In particular, Fig. 9 testifies that normal modes of BPS mechanical kinks are not prepared to approximate the shape mode of the ϕ^4 kink even for very high N. This could be an important clue. Coupled with the observation of the dynamical instability of $N > 1$ BPS mechanical kinks, we may conclude that there is a conceptual difference between kinks and mechanical kinks that persists for any N. One difference that indeed persists is the compactness of the mechanical field. Thus, it may not be enough just to increase N to reach a quantitative match with field theory, but some new ingredient might be needed.

The dynamical instability observed in both non-BPS and BPS mechanization might be simply an artifact of our choice of CCM. A similar circumstance was reported in [28] in the context of the discretized nonlinear Schrödinger equation. There the authors observed a spurious instability that originated from their choice of collective coordinates, which was then resolved by adopting a broader *Ansatz*.

In the context of mechanization, the presence or absence of joint ejections might therefore serve as a useful discrimination tool among various piecewise *Ansätze* that we may consider. In addition, the distribution of normal modes of mechanical kinks could also constitute an independent gauge for a *post hoc* validation of the selected CCM. Investigation of the phenomenon of joint ejections and distribution of normal modes of mechanical kinks for various piecewise *Ansätze* is left for future work.

The compactness of mechanical fields is also the reason for introducing the second conceptual advancement. In the pursuit of direct mechanical-$K\bar{K}$ scattering, we have shown that short-range interactions in field theory can be replaced by contact interactions by allowing joints to pass through each other. This can be achieved without encountering singularities, which are present in a general mechanical field, by working with constrained mechanical fields. Fortunately, a mechanical-$K\bar{K}$ pair separated by a flat segment of length $R > 0$ is such a mechanical field whose moduli space is regular at $R = 0$ and we may continue the dynamics for negative values $R < 0$ via switching to a (constrained) mechanical oscillon as described in Sec. IV. This is embodied in the notion of loose order mechanization.

First, we presented a LOM for rigid mechanical-$K\bar{K}$ scattering, where only the separation R is dynamic. There the LOM involves four stages (see Fig. 12) that cover the full range of the moduli $R \in (-\infty, \infty)$. When we turned on the time dependence of widths, $R_K(t)$, we encountered a singularity at the transition from the second stage to the third, preventing the mechanical field from going below the vacuum. The same problem, known as the null-vector problem, appears also in naive CCMs and can be overcome by including more moduli [10]. In our approach too we expect the null-vector problem to go away when we increase the number of joints.

It is surprising that both the BPS property and the necessity of LOM point to the same conclusion: A generic mechanical field has too many degrees of freedom and it needs to be constrained. This is perhaps not surprising, given the *ad hoc* nature of its construction. In particular, during the course of dynamical evolution, the $N > 1$ BPS mechanical kinks easily shed degrees of freedom via joint ejections. This, in restricted capacity, is true also for non-BPS mechanical kinks and it

has been observed in high-N mechanical oscillons as well [22]. The construction of LOM, which consists in joining together effective Lagrangians for different orderings of the joints, would not work at all if we allow all moduli of a generic mechanical field to be dynamic.

As a closing remark, however, let us also point out a case where the problem could be the exact opposite. Indeed, if we consider a free-field theory with $V = 0$, a general solution is described by superposition of arbitrary shapes moving with the speed of light to either the left or the right: $\phi_{\text{free}}(x,t) = f_{\text{L}}(x-t) + f_{\text{R}}(x+t)$. As a corollary, the solution to the Cauchy problem with a static initial shape, i.e., $\phi_{\text{free}}(x,0) = f(x)$ and $\dot{\phi}_{\text{free}}(x,0) = 0$, is described by an immediate disintegration into two copies of the same shape with half the amplitude: $\phi_{\text{free}}(x,t) = f(x-t)/2 + f(x+t)/2$.

In the mechanized version of the free-field theory, this does not happen. Starting with a symmetric $N = 2$ mechanical field, a triangle of width R and height A, the governing equations of motion

$$\ddot{R} = \frac{16}{R} - \frac{2\dot{A}\dot{R}}{A}, \quad \ddot{A} = A\frac{\dot{R}^2}{R^2} - \frac{20A}{R^2} \tag{78}$$

can be solved exactly as

$$R = R_0 + 4t, \quad A = A_0\sqrt{1 + 4t/R_0}, \tag{79}$$

which depicts an ever-expanding triangle with a constant static mass $A^2/R = A_0^2/R_0$. Clearly, such a solution is unphysical, not just because the joints fly apart with twice the speed of light. The correct solution should be the same as in field theory, that the triangle disintegrates into two similar triangles with half the initial height, flying apart with the speed of light. However, this would require an instantaneous transition from a symmetric $N = 2$ mechanical field with three joints to a symmetric $N = 5$ mechanical field with six joints. In other words, there would be a (triple) bifurcation at $t = 0$ where each joint turns into two. Also note that such a bifurcation would be a relativistic effect. We believe that some strange characteristics of mechanical kinks dynamics can be potentially explained by the current lack of a bifurcation process, which should be investigated in future work.

ACKNOWLEDGMENTS

We would like to thank T. Romańczukiewicz and A. Wereszczyński for many fruitful discussions and help with the numerical code. We also acknowledge the institutional support of the Research Centre for Theoretical Physics and Astrophysics, Institute of Physics, Silesian University in Opava.

[1] N. S. Manton and P. Sutcliffe, *Topological Solitons* (Cambridge University Press, Cambridge, 2004).
[2] A. Vilenkin and E. P. S. Shellard, *Cosmic Strings and Other Topological Defects* (Cambridge University Press, Cambridge 2000).
[3] Y. M. Shnir, *Topological and Non-Topological Solitons in Scalar Field Theories*, Cambridge Monographs on Mathematical Physics (Cambridge University Press, 2018).
[4] T. Sugiyama, Kink-antikink collisions in the two-dimensional ϕ^4 model, Prog. Theor. Phys. **61**, 1550 (1979).
[5] D. K. Campbell, J. F. Schonfeld, and C. A. Wingate, Resonance structure in kink-antikink interactions in ϕ^4 theory, Physica D **9**, 1 (1983).
[6] M. Moshir, Soliton-anti-soliton scattering and capture in $\lambda\phi^4$ theory, Nucl. Phys. B **185**, 318 (1981).
[7] T. I. Belova and A. E. Kudryavtsev, Quasi-periodic orbits in the scalar classical $\lambda\phi^4$ field theory, Physica D **32**, 18 (1988).
[8] P. Anninos, S. Oliveira, and R. A. Matzner, Fractal structure in the scalar $\lambda(\phi^2-1)^2$ theory, Phys. Rev. D **44**, 1147 (1991).
[9] N. S. Manton, K. Oleś, T. Romańczukiewicz, and A. Wereszczyński, Kink moduli spaces: Collective coordinates reconsidered, Phys. Rev. D **103**, 025024 (2021).
[10] N. S. Manton, K. Oles, T. Romanczukiewicz, and A. Wereszczynski, Collective coordinate model of kink-antikink collisions in ϕ^4 theory, Phys. Rev. Lett. **127**, 071601 (2021).
[11] C. Adam, N. S. Manton, K. Oles, T. Romanczukiewicz, and A. Wereszczynski, Relativistic moduli space for kink collisions, Phys. Rev. D **105**, 065012 (2022).
[12] P. Dorey, K. Mersh, T. Romanczukiewicz, and Y. Shnir, Kink-antikink collisions in the ϕ^6 model, Phys. Rev. Lett. **107**, 091602 (2011).
[13] C. Adam, P. Dorey, A. G. Martín-Caro, M. Huidobro, K. Oles, T. Romanczukiewicz, Y. Shnir, and A. Wereszczynski, Multi-kink scattering in the ϕ^6 model revisited, Phys. Rev. D **106**, 125003 (2022).
[14] H. Weigel, Kink-antikink scattering in φ^4 and ϕ^6 models, J. Phys.: Conf. Ser. **482**, 012045 (2014).
[15] P. Dorey, A. Gorina, T. Romańczukiewicz, and Y. Shnir, Collisions of weakly-bound kinks in the Christ-Lee model, J. High Energ. Phys. 09 (2023) 45.
[16] C. Adam, C. Halcrow, K. Oles, T. Romanczukiewicz, and A. Wereszczynski, Moduli space for kink collisions with moving center of mass, SIGMA **19**, 054 (2023).
[17] C. Adam, D. Ciurla, K. Oles, T. Romanczukiewicz, and A. Wereszczynski, Relativistic moduli space and critical velocity in kink collisions, Phys. Rev. E **108**, 024221 (2023).
[18] P. G. Kevrekidis and R. H. Goodman, Four decades of kink interactions in nonlinear Klein-Gordon models: A crucial typo, recent developments and the challenges ahead, arXiv:1909.03128
[19] P. Dorey and T. Romańczukiewicz, Resonant kink-antikink scattering through quasinormal modes, Phys. Lett. B **779**, 117 (2018).
[20] C. Adam, K. Oles, T. Romanczukiewicz, and A. Wereszczynski, Spectral walls in soliton collisions, Phys. Rev. Lett. **122**, 241601 (2019).

[21] C. Adam, K. Oles, T. Romanczukiewicz, and A. Wereszczynski, Spectral walls in antikink-kink scattering in the ϕ^6 model, Phys. Rev. D **106**, 105027 (2022).

[22] F. Blaschke and O. N. Karpíšek, Mechanization of scalar field theory in 1+1 dimensions, Prog. Theor. Exp. Phys. **2022**, 103A01 (2022).

[23] E. B. Bogomolny, Stability of classical solutions, Sov. J. Nucl. Phys. **24**, 449 (1976).

[24] H. Arodz, Topological compactons, Acta Phys. Pol. B **33**, 1241 (2002).

[25] H. Arodz, P. Klimas, and T. Tyranowski, Compact oscillons in the signum-Gordon model, Phys. Rev. D **77**, 047701 (2008).

[26] F. M. Hahne, P. Klimas, J. S. Streibel, and W. J. Zakrzewski, Scattering of compact oscillons, J. High Energy Phys. 01 (2020) 006.

[27] I. C. Christov, R. J. Decker, A. Demirkaya, V. A. Gani, P. G. Kevrekidis, and R. V. Radomskiy, Long-range interactions of kinks, Phys. Rev. D **99**, 016010 (2019).

[28] R. Rusin, R. Kusdiantara, and H. SusantoVariational approximations using Gaussian ansatz, false instability, and its remedy in nonlinear Schrödinger lattices, J. Phys. A: Math. Theor. **51**, 475202 (2018).